

Phenomenological model for history effects and metastability in weakly pinned superconductors

G. Ravikumar,* K. V. Bhagwat, and V. C. Sahni

Technical Physics and Prototype Engineering Division, Bhabha Atomic Research Centre, Mumbai 400 085, India

A. K. Grover and S. Ramakrishnan

Tata Institute of Fundamental Research, Mumbai 400 005, India

S. Bhattacharya[†]

*NEC Research Institute, 4 Independence Way, Princeton, New Jersey 08540
and Tata Institute of Fundamental Research, Mumbai 400 005, India*

(Received 20 October 1999)

We present a phenomenological model to describe features in the hysteretic magnetic response of weak pinning superconductors across the peak effect region. It accounts for the experimentally observed history dependent behavior of critical current density and the metastability of the vortex state prior to and across the peak effect region of superconducting systems such as NbSe₂, CeRu₂, and YBa₂Cu₃O₇. Moreover, this model reduces to Bean's critical state model as a limiting case.

The hysteretic magnetic response of a type-II superconductor provides a measure of pinning of the vortex state. It is traditionally described by Bean's critical state model¹ (CSM) in commonly encountered situations where the pinning property is uniquely determined by the magnetic field value at a fixed temperature. But it fails to even qualitatively account for the recent experimental observations in weak pinning samples of systems such as NbSe₂, CeRu₂, YBa₂Cu₃O₇, Ca₃Rh₄Sn₁₃, etc.,²⁻⁵ that exhibit a pronounced peak effect (PE). In this paper we propose a model that accounts for all the features of the hysteretic magnetic response described below.

The phenomenon of PE is the occurrence of an anomalous peak in J_c vs H at a field H_p just below the upper critical field H_{c2} . Within the Larkin-Ovchinnikov collective pinning theory,⁶ the increase in J_c signifies a decrease in the correlation volume V_c over which the vortex lattice (VL) remains correlated. In other words, VL undergoes an order to disorder transformation across the PE region.^{2,7} A variety of anomalous behavior is observed in this region: (1) The magnetization M vs field H curve measured in the field increasing cycle (forward curve) and that in the field decreasing cycle (reverse curve), which constitute the so-called envelope loop, are highly asymmetric in the peak region.⁸ (2) Ravikumar *et al.*² studied the magnetic response of weakly pinned VL in single crystals of NbSe₂ and CeRu₂ by varying the field after cooling the sample in a field $H < H_p$ (the field cooled or FC state). Surprisingly, the change in field causes the magnetization values to *overshoot* the envelope magnetization curve. A subsequent change in field causes the magnetization values lying outside the envelope loop to gradually return towards the envelope curve. (3) Furthermore, the minor curves starting from a point ($H < H_p$) on the forward curve *saturate without meeting the reverse curve*, although they remain well within the hysteresis envelope.³⁻⁵ (4) On the other hand, the minor curves starting from a point ($H < H_p$) on the reverse curve *overshoot* the forward branch of the envelope.³

These observations cannot be understood within the framework of CSM and indicate that J_c is magnetic history dependent over a large part of (H, T) space.^{3,9-11} In what follows we describe a phenomenological model that accounts for all the above violations of standard CSM.

The field distribution in a superconductor is described by Maxwell's equation $\nabla \times \mathbf{B} = \mu_0 \mathbf{J}$, where $\mu_0 = 4\pi \times 10^{-7}$ and \mathbf{B} and \mathbf{J} are the local-field and current distributions, respectively. For simplicity, we consider a superconducting slab, extending from 0 to $2a$ in x dimension and infinite in y and z dimensions. The field profile $B(x, H)$ at an external field H along the z axis is symmetric about $x = a$ and we therefore confine the discussion to the region $0 < x < a$. $B(x, H)$ is now determined by $\partial B(x, H)/\partial x = -\mu_0 J$ with the current density J parallel to the y axis. In the standard CSM, $J = \pm J_c$, when $B \neq 0$, and $J = 0$, when $B = 0$. The upper (lower) sign is applicable on the forward (reverse) curve. Moreover, J_c (positive) is uniquely determined by B at a given temperature T . The limiting values of magnetization M are $-\mu_0 J_c a/2$ and $\mu_0 J_c a/2$ on the forward and reverse curves, respectively. All possible isothermal magnetization values should lie within these limiting values. This is clearly violated in the PE region of weak pinning superconductors as discussed above. In view of the inadequacy of the CSM in such situations, we propose the following model which reduces to CSM as a special case.

We consider the field profile $B(x, H)$ at an external field H which is governed by

$$\partial B(x, H)/\partial x = \mp \mu_0 J_c. \quad (1)$$

When the external field is increased (decreased) by an infinitesimal quantity δH , the field profile is altered to $B(x, H \pm \delta H)$, which corresponds to a new current distribution J'_c determined by

$$\partial B(x, H \pm \delta H)/\partial x = \mp \mu_0 J'_c. \quad (2)$$

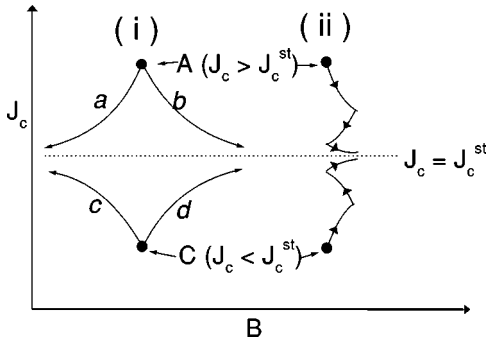


FIG. 1. Approach of the current density J_c towards J_c^{st} given by Eq. (3) is schematically shown as a function of field B for a fixed J_c^{st} . (i) At point A, $J_c > J_c^{st}$ and J_c decreases when the field is increased (path b) or decreased (path a). Similarly, at point C, $J_c < J_c^{st}$ and J_c increases when the field is increased (path d) or decreased (path c). (ii) The same is shown under the application of an oscillatory field.

To allow for the history dependence in the J_c , we propose the following new form for J'_c , which is central to our model

$$J'_c = J_c + (|\Delta B|/B_r)(J_c^{st} - J_c). \quad (3)$$

The parameters J_c^{st} (stable current density) and B_r (retardation parameter) are only assumed to be uniquely determined by B and T . ΔB is the change in local field B for an infinitesimal variation $\pm \delta H$ in the external field.

Let us now examine the consequences of Eq. (3). First, it allows J_c to depend on the magnetic history of the system, thereby lifting the restriction on the uniqueness of J_c imposed in CSM. Second, J_c can be different from J_c^{st} but such a state is metastable. The metastable J_c is driven to its stable value J_c^{st} by a change in the local field B , independent of its sign, as ensured by the absolute value $|\Delta B|$ in Eq. (3). This evolution of J_c is shown schematically in section (i) of Fig. 1, when initial J_c is both greater and less than J_c^{st} and for both increasing and decreasing B from the ambient value in each case. Additionally, section (ii) of Fig. 1 shows a similar approach to J_c^{st} , when the field is cycled. Physically, we may imagine that in the absence of thermal fluctuations it is the change in local field B that can move the vortices from their metastable configuration. It could be considered as another mechanism in addition to the current driven reorganization of the vortices from the metastable vortex state elucidated by Paltiel *et al.*¹² in a more strongly pinned sample of NbSe₂. Third, this model reduces to the usual CSM in the limit $B_r = 0$, i.e., $J'_c = J_c = J_c^{st}$ (in order that J_c and J'_c remain finite). Thus, in our model, J_c^{st} represents a unique parameter describing the pinning property of the stable state, i.e., the role played by J_c in CSM. B_r is a macroscopic measure of the metastability at a given field. We expect it to depend on the competition between elastic and pinning energies. When elasticity dominates (i.e., H far below the peak regime) or when pinning dominates (i.e., $H > H_p$) we expect B_r to be small (zero). But when the two energies are comparable (as in the PE region) and, moreover, thermal fluctuations are inadequate, B_r is large implying a large free-energy (energy as well as entropy) barrier between the ordered and disordered phases.

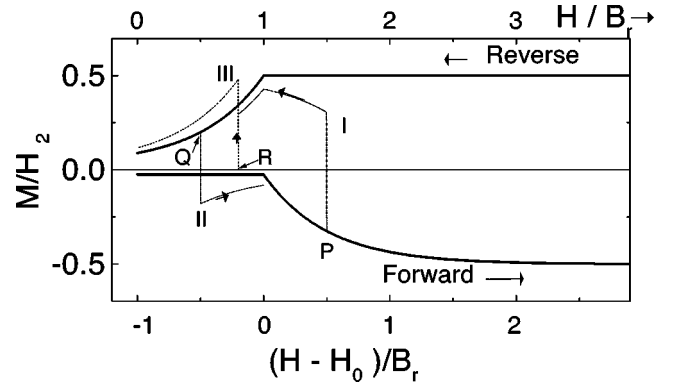


FIG. 2. Normalized magnetization curves on the forward and reverse field cycles. For $H > H_0$ ($H < H_0$) on the forward (reverse) curve, magnetization approaches the standard CSM value $-H_2^*/2(H_1^*/2)$ asymptotically. We assumed $H_2^*/H_1^* = J_2/J_1 = 20$. The minor curve (I) obtained by decreasing the field from the point P on the forward curve saturates without merging with the reverse curve. The minor curve (II) obtained by increasing the field from the point Q on the reverse curve overshoots the forward envelope curve. The minor curve (III) obtained by decreasing the field from point R ($M_{FC} = 0$) corresponding to the FC state at $H < H_0$ overshoots the reverse curve. The minor curves are calculated with $4\pi B_r/H_2^* = 2.5 \times 10^3$. In Bean's model ($B_r \rightarrow 0$), the minor curves remain within the forward and reverse curves.

Using the form of J'_c [cf. Eq. (3)] in Eq. (2) and using Eq. (1) we get

$$\partial|\Delta B|/\partial x = -|\Delta B|[\mu_0 J_c^{st} \pm \partial B(x, H)/\partial x]/B_r. \quad (4)$$

We note that $|\Delta B| = B(x, H + \delta H) - B(x, H)$ in the forward case and $|\Delta B| = B(x, H) - B(x, H - \delta H)$ in the reverse case. Integrating Eq. (4) from 0 to x with the boundary condition, $|\Delta B(x=0)| = \mu_0 \delta H$, and passing through the limit $\delta H \rightarrow 0$, we obtain

$$(1/\mu_0)\partial B(x, H)/\partial H = \exp[\{-\mu_0 J_c^{st} x \mp B(x, H) \pm \mu_0 H\}/B_r]. \quad (5)$$

Knowing the initial profile $B(x, H_0)$ at some field H_0 , the profile $B(x, H)$ can be determined from Eq. (5) at all subsequent H . J_c^{st} and B_r are assumed to be slowly varying functions of B and treated as constants (depending on the applied field H) while integrating Eq. (4).

First, we consider a simple case, where B_r is independent of field and $J_c^{st} = J_1$ for $H < H_0$ and $J_c^{st} = J_2 (> J_1)$ for $H > H_0$. This mimics the sharp jump in J_c , when the VL changes from an ordered to a disordered state across the peak region.⁷ This simple case is analytically solvable and the details will be published elsewhere. In the forward case, for fields $H \leq H_0$, the system can be prepared in the state with a stable current density J_1 (as described in Fig. 1) corresponding to the field profile $B(x, H) = \mu_0(H - J_1 x)$. For subsequent fields on the forward cycle, the field profile evolves according to Eq. (5) with the upper sign. Similarly, on the reverse cycle, the field profile at some $H > H_0$ can be prepared in a state with the stable current density J_2 , corresponding to the field profile $B(x, H) = \mu_0(H + J_2 x)$. For decreasing field on the reverse cycle, the field profile is obtained by solving Eq. (5) with lower sign. M is determined

using $M(H) = (1/a) \int_0^a B(x, H) dx - \mu_0 H$. The integration of the field profiles is carried out numerically. Magnetization M (normalized by $H_2^* = \mu_0 J_2 a$) on the forward and reverse field cycles is plotted in Fig. 2 as a function of H (normalized by B_r). For large H , M on the forward cycle approaches the limiting value $-H_2^*/2$ corresponding to $J_c = J_2$. As the field is reduced well below H_0 on the reverse cycle, M approaches the limiting value $H_1^*/2 = \mu_0 J_1 a/2$.

Let us now discuss the minor magnetization curves. When the external field is decreased (increased) from a given value on the forward (reverse) curve, the field profile is calculated in the spirit of critical state model. To the lowest order, the sign of the local current density J_c reverses, when the sense of local field change is reversed.¹ The local-field change ΔB further contributes a term that drives the current density J_c closer to J_c^{st} [cf. Eq. (3)]. The minor magnetization curve I (II) obtained by integrating the field profiles in the case of field decreasing (increasing) from a point $P(Q)$ on the forward (reverse) cycle is also presented in Fig. 2. The minor curve (I) initiated from the forward curve saturates without meeting with the reverse curve,³⁻⁵ while the minor curve (II) initiated from the reverse curve overshoots the forward curve just as seen in experiments.³

We now consider a superconductor cooled in a field $H_{FC} < H_0$ (cf. point R in Fig. 2). The initial field profile in the FC case can be assumed to be uniform with zero shielding currents. An infinitesimal change in the local field $\mu_0 H^{FC}$ induces a shielding current J_c^{FC} . A further change in the local field drives this current closer to J_c^{st} [cf. Eq. (3)]. From experiments we know that FC state has a critical current density J_c^{FC} which is higher than that on both the increasing and decreasing field cycles.^{2,9-11} Implementing this idea, we calculated the field profile for decreasing external field from the value H_{FC} . We have chosen $J_c^{FC}(H < H_0) = J_2$ signifying the supercooled disordered state of vortex lattice.^{3,9} In Fig. 2, we present the M vs H curve (III) obtained by decreasing the field from the FC state, which mimics the experimental results.

Having thus established the qualitative agreement between the results of our model and those in recent experiments, we apply this model to a specific case, i.e., in the PE region of NbSe₂ at a given temperature (6.95 K) with a more detailed parametrization than in the idealized case described above. Below some field H_{low} and above H_p , the minor curves are observed³ to conform to the CSM, implying the absence of history dependence in J_c . This also amounts to B_r being zero for these field ranges. The history dependence is observed in the intermediate fields ($H_{low} < H < H_p$), and to account for this we assume $B_r \propto (H - H_{low})^2 (H_p - H)^2$. To obtain a semiquantitative understanding of our data, we further parametrize J_c^{st} in the following form:

$$J_c^{st}(H) = J_{c1}(1 - H/H_1) + J_{c2}e^{-(H-H_p)^2/2H_w^2}. \quad (6)$$

The second term on the right-hand side of Eq. (6) reflects the peak in J_c^{st} vs H . The choice of the above specific forms for B_r and J_c^{st} is not unique. But the conclusions are not crucially dependent on this choice.

We now consider the initial field profile $B(x, H_0 < H_{low}) = \mu_0[H_0 - J_c^{st}(H_0)x]$ applicable in the forward cycle. Solv-

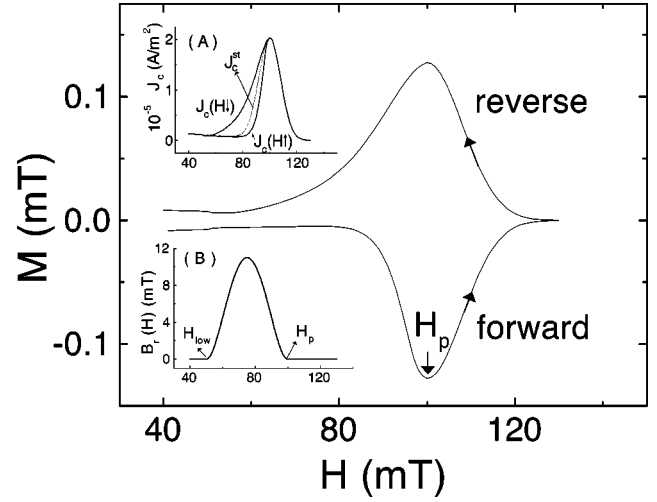


FIG. 3. Magnetization hysteresis loop calculated with $H_{low} = 0.05T$, $H_p = 0.1T$, $J_{c1} (=10^4 \text{ A/m}^2)$, $J_{c2} (=20J_{c1})$, $H_1 (=0.12T)$, and $H_w (=0.008T)$. Inset A shows the field dependence of the J_c on the forward ($H \uparrow$) and reverse ($H \downarrow$) field cycles determined from the hysteresis loop obtained using the model. These are compared with the J_c^{st} given by Eq. (6). Inset B shows the field dependence of the retardation parameter B_r used in the calculation.

ing Eq. (5) numerically (with upper sign), we obtain the field profile $B(x, H)$ for $H > H_0 (=0.04T)$. Similarly, in the reverse cycle, we start with an initial state at a field $H_0 (=0.13T) > H_p$, where again the field profile is uniquely determined by CSM $\{B(x, H_0) = \mu_0[H_0 + J_c^{st}(H_0)x]\}$, and obtain $B(x, H)$ for $H < H_0$ by numerically solving Eq. (5) (with lower sign). In insets A and B of Fig. 3 we show the $J_c^{st}(H)$ [cf. Eq. (6)] and $B_r(H)$, respectively. The forward and reverse magnetization curves are obtained from the integral of field profiles $B(x, H)$. They are plotted in the main panel of Fig. 3. It compares very well to the experimentally measured hysteresis loop [see Fig. 4(c)] of an NbSe₂ crystal at 6.95 K. *The usually observed asymmetric nature of hysteresis loop in the PE region is clearly brought out by this model.* To further analyze the asymmetry, we plot in the inset A of Fig. 3, $-M(H \uparrow)/\mu_0 a$ and $M(H \downarrow)/\mu_0 a$, which

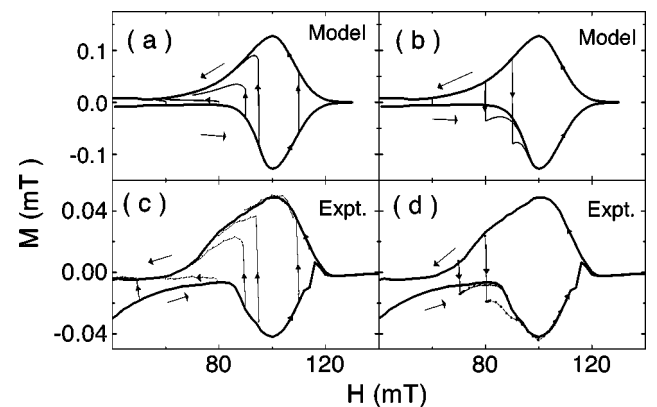


FIG. 4. Calculated minor curves initiated from different points ($H < H_p$) lying on the (a) forward curve and (b) the reverse curve. They are compared with the experimental data on the NbSe₂ crystal at 6.95 K with $H \parallel c$ shown in (c) and (d), respectively. The envelope loop has also been shown in each of the figures.

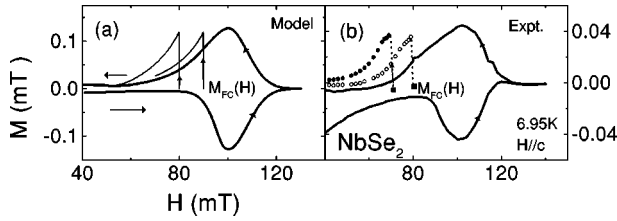


FIG. 5. (a) Calculated minor curves obtained by decreasing the field after field cooling (in $H_{FC} < H_p$) the system. They are compared with the experimental data shown in (b).

signify the J_c values on the forward and the reverse cycles, respectively. These are compared with the $J_c^{st}(H)$ originally assumed in the model [Eq. (6)]. From the inset A of Fig. 3 it is clear that the induced currents on the forward (reverse) cycle tend to remain lower (higher) than the stable value J_c^{st} in the field region $H_{low} < H < H_p$, thus reflecting the history dependence in J_c as seen in experiments.^{3,10}

In Fig. 4(a) [Fig. 4(b)], the calculated minor curves obtained by decreasing (increasing) the field from forward (reverse) curves, using the ideas discussed earlier, are compared with the relevant experimental data in NbSe₂ crystal shown in Fig. 4(c) [Fig. 4(d)]. Finally, we display in Fig. 5(a) the calculated minor curves with a field cooled state as the initial

state. Recalling that a given FC state has a higher critical current than the stable value at that field, we assume $J_c^{FC} = J_{c2}$ for $H_{low} < H < H_p$. The calculated results in Fig. 5(a) are in excellent agreement with the experimental data shown in Fig. 5(b).

To conclude, we have presented a model for explaining the features in history dependent magnetization (minor curves) observed in the peak effect region in various superconducting systems such as NbSe₂, CeRu₂, and YBa₂Cu₃O₇. In this model we have postulated the existence of a stable critical current value J_c^{st} and the retardation parameter B_r , which are unique for a given field and temperature. Our results indicate that the critical currents obtained by commonly used magnetic histories [viz., in increasing and decreasing field cycles, field cooled (FC) case, etc.] correspond to different metastable states of the vortex lattice with varying degrees of lattice correlations. The success of the model in reproducing the experimental results attests to its usefulness. It remains to be seen if microscopic models can provide a basis for the phenomenological model described here and thus a more detailed understanding of the metastability seen in experiments as well as in this model.

The authors are grateful to Professor Deepak Dhar for discussions.

*Electronic address: gurazada@apsara.barc.ernet.in

†Electronic address: shobo@research.nj.nec.com

¹C.P. Bean, Phys. Rev. Lett. **8**, 250 (1962); Rev. Mod. Phys. **36**, 31 (1964).

²G. Ravikumar *et al.*, Phys. Rev. B **57**, R11 069 (1998).

³G. Ravikumar *et al.*, cond-mat/9908222, Phys. Rev. B (to be published 1 May 2000).

⁴S.B. Roy and P. Chaddah, J. Phys.: Condens. Matter **9**, L625 (1997).

⁵S. Kokkaliaris *et al.*, Phys. Rev. Lett. **82**, 5116 (1999); S. Sarkar *et al.*, cond-mat/9909297, Phys. Rev. B (to be published 1 May 2000).

⁶A.I. Larkin and Y.N. Ovchinnikov, J. Low Temp. Phys. **34**, 409

(1979); A.I. Larkin, Zh. Éksp. Teor. Fiz. **31** 1466 (1970) [Sov. Phys. JETP **31**, 784 (1970)].

⁷P.L. Gammel *et al.*, Phys. Rev. Lett. **80**, 833 (1998); S.S. Banerjee *et al.*, Phys. Rev. B **59**, 6043 (1999).

⁸G. Ravikumar *et al.*, Physica C **298**, 122 (1998).

⁹W. Henderson *et al.*, Phys. Rev. Lett. **77**, 2077 (1996).

¹⁰M. Steingart, A.G. Putz, and E.J. Kramer, J. Appl. Phys. **44**, 5580 (1973).

¹¹R. Wordenweber, P.H. Kes, and C.C. Tsuei, Phys. Rev. B **33**, 3172 (1986).

¹²Y. Paltiel *et al.*, cond-mat/9912157, Nature (London) (to be published).